Journal of Bioscience and Bioengineering
VOL. 127 No. 3, 301–308, 2019

www.elsevier.com/locate/jbiosc

Metabolome analysis revealed the knockout of glyoxylate shunt as an effective strategy for improvement of 1-butanol production in transgenic *Escherichia coli*

Katsuaki Nitta,[1] Walter A. Laviña,[1,2] Sammy Pontrelli,[3] James C. Liao,[3] Sastia P. Putri,[1,*] and Eiichiro Fukusaki[1]

Department of Biotechnology, Graduate School of Engineering, Osaka University, 2-1 Yamadaoka, Suita, Osaka 565-0871, Japan,[1] Department of Microbiology, Institute of Biological Sciences, College of Arts and Sciences, University of the Philippines Los Baños, College, 4031 Laguna, Philippines,[2] and Department of Chemical and Biomolecular Engineering, University of California, Los Angeles, 5531 Boelter Hall, 420 Westwood Plaza, Los Angeles, CA 90095, USA[3]

Received 22 March 2018; accepted 28 August 2018
Available online 25 October 2018

High 1-butanol titer has been achieved in a transgenic *Escherichia coli* strain JCL299FT with a heterologous 1-butanol pathway by deleting competing pathways, balancing of cofactor and resolving free CoA imbalance. However, further improvement of 1-butanol production is still possible in the highest producing strain JCL299FT as indicated by the accumulation of acetate, a major undesired by-product during bio-production by microorganisms that competes with 1-butanol production for the available acetyl-CoA and inhibits protein synthesis resulting in poor growth. In this study, liquid chromatography/tandem mass spectrometry (LC/MS/MS)-based metabolome analysis was performed to identify new rate limiting steps in the 1-butanol production pathway of *E. coli* strain JCL299FT. The results of metabolome analysis showed increased amounts of glyoxylate in JCL299FT compared to the previous highest-producing strain JCL299F. Knocking out *aceA* successfully decreased the amount of glyoxylate and reduced acetate accumulation, resulting in the increased levels of TCA cycle and 1-butanol pathway metabolites. These observations indicated that there was a redirection of flux from acetate to TCA cycle and 1-butanol producing pathway, which led to better growth of the 1-butanol producing strain. Consequently, 1-butanol production titer was improved by 39% and the production yield was improved by 12% in M9 medium supplemented with yeast extract. This study is the first report of using the knockout of *aceA*, the first gene in the glyoxylate shunt that encodes isocitrate lyase, as an effective strategy to reduce acetate overflow in 1-butanol producing *E. coli*.

[**Key words:** Metabolomics; *Escherichia coli*; 1-Butanol; Glyoxylate shunt; Strain improvement]

Metabolomics is the high-resolution phenotype analysis of biological samples via the comprehensive examination of metabolites in the sample (1). Recently, metabolomics has been used for metabolic engineering studies where strain improvement for increased production of useful compounds is desired (2–5). In such cases, metabolomics was used to provide a deeper insight in the cellular metabolism of the organism, which can be applied to identify non-obvious gene targets for strain improvement and increased production. Our group successfully demonstrated the power of metabolomics in metabolic engineering studies by revealing important metabolome phenomena and improving 1-butanol production in microorganisms such as the cyanobacteria *Synechococcus elongatus* (6) and *Escherichia coli* (7).

1-Butanol is a bulk chemical and promising biofuel that can replace gasoline and potentially promote a sustainable society upon production improvement. Previously, *E. coli* has been engineered to produce 1-butanol using a modified *Clostridial* CoA-dependent production pathway (8). Previously reported production strains have been subjected to several modifications. A base strain, designated as JCL299F (*ΔldhA ΔadhE ΔfrdBC Δpta* with expression of the 1-butanol pathway), is deficient in all native fermentation pathways, and thus, growth in anaerobic conditions is coupled to production as the strain relies on 1-butanol formation as the sole electron sink to regenerate NAD^+ (9). Deletion of *pta*, phosphate acetyltransferase, prevents byproduct formation of acetate to enhance flux of carbon through the pathway and raised butanol titers to 15 g/L after 72 h of production in rich medium (9). Expression of AdhE2 was optimized in the JCL299F strain (now designed as JCL299FT) to enable efficient CoA recycling of the pathway, which resulted in the increase of 1-butanol titers up to 18.3 g/L with cysteine supplementation in rich medium after 78 h (7). The genetic background of each strain and heterologous genes for 1-butanol production is shown in Fig. 1 and Table 1. However, JCL299FT still shows acetate accumulation (around 4 g/L for 24 h cultivation in TB medium) (10) even though the main gene that catalyzes the reaction from acetyl-phosphate to acetate (*pta*) has been deleted (7–10). Acetate accumulation inhibits protein synthesis (11) and competes with 1-butanol pathway for the use of acetyl-CoA. Therefore, acetate production needs to be decreased in order to further improve growth and 1-butanol production. In an attempt to alleviate this accumulation, we over-expressed *atoB*, which encodes the first enzyme in the 1-butanol producing pathway,

* Corresponding author. Tel./fax: +81 6 6879 7416.
E-mail addresses: katsuaki_nitta@bio.eng.osaka-u.ac.jp (K. Nitta), walavina@up.edu.ph (W.A. Laviña), sppontrelli@gmail.com (S. Pontrelli), liaoj@ucla.edu (J.C. Liao), sastia_putri@bio.eng.osaka-u.ac.jp (S.P. Putri), fukusaki@bio.eng.osaka-u.ac.jp (E. Fukusaki).

1389-1723/$ – see front matter
https://doi.org/10.1016/j.jbiosc.2018.08.013

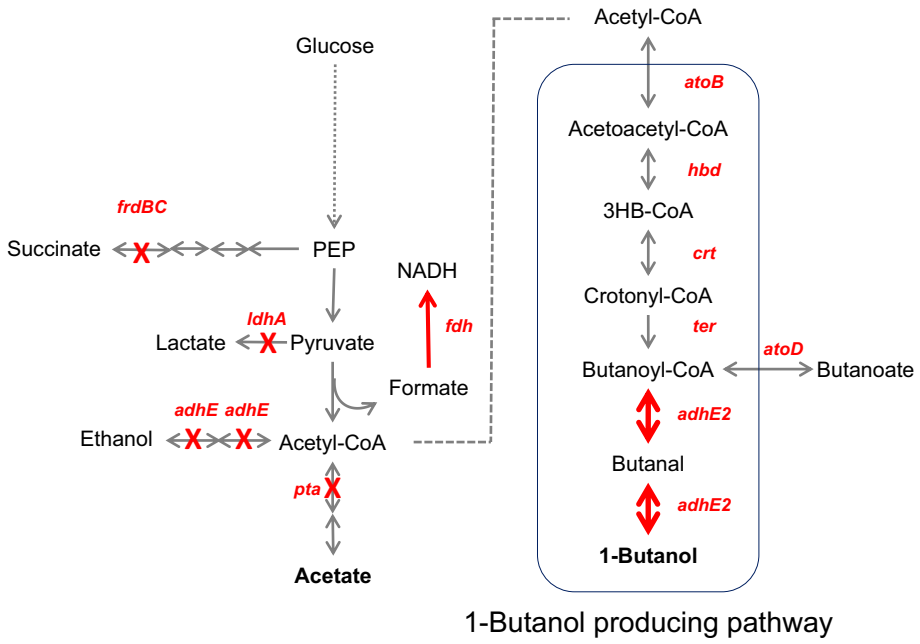

FIG. 1. Metabolic pathway in this work. X marks indicate gene knockouts. Thick, red arrows indicate over-expression of enzymes. Gene abbreviations: *frdBC*, fumarate reductase; *adhE*, alcohol dehydrogenase; *ldhA*, lactate dehydrogenase; *fdh*, formate dehydrogenase; *pta*, phosphate transferase; *atoB*, acetyl-CoA acetyl transferase; *hbd*, 3-hydroxybutanoyl-CoA dehydrogenase; *crt*, crotonase, *ter*, *trans*-enoyl-CoA reductase; *adhE2*, aldehyde/alcohol dehydrogenase; *atoD*, acetoacetyl-CoA transferase (*atoD*). *fdh* was introduced from *Candida boidinii*. *hbd*, *crt* and *adhE2* were introduced from *Clostridium acetobutylicum*. *ter* was introduced from *Treponema denticola*.

to pull the carbon flux into the 1-butanol producing pathway resulting in the improvement of 1-butanol production (10). Other strategies to improve production include increasing precursor availability and removal of competing pathways. In a previous study, *eutD*, which encodes the isozyme of *pta* was deleted. Consequently, a decrease in acetate production with a corresponding increase in acetyl-CoA, a 1-butanol precursor, was successfully achieved. However, unexpected pyruvate accumulation and a decrease in 1-butanol production were also observed (10).

In this study, metabolome analysis was employed to identify new gene targets to increase 1-butanol production by comparing the metabolomic measurements of the production strains. Metabolome analysis revealed an accumulation of glyoxylate in JCL299FT compared to the previous strain JCL299F. In our previous study, deletion of *eutD* in JCL299FT resulted in lower 1-butanol production (10). Here, deletion of *aceA*, which encodes the first enzyme of glyoxylate shunt, not only led to a decreased level of glyoxylate but also decreased level of acetate. More importantly, it resulted in better growth and a 39% improvement in 1-butanol production when cultivated in M9 + YE (yeast extract) medium. This work demonstrates that knocking out *aceA* is an effective strategy for diverting flux of the TCA cycle and decreasing acetate production, consequently increasing 1-butanol production.

TABLE 1. *E. coli* strains, plasmids and primers used in the study.

Strain/Plasmid/Primer	Relevant characteristics	Source
E. coli strain		
JCL16	BW25113/F' [Δ*traD*36 *proAB*$^+$ Δ*lacI*^{q}ZΔM15 (Tet^r)]	Atsumi et al. (8)
JCL299	JCL16 Δ*ldhA* Δ*adhE* Δ*frdBC* Δ*pta*	Atsumi et al. (8)
JCL306	JCL16 Δ*ldhA* Δ*adhE* Δ*frdBC* Δ*pta* Δ*eutD*	Nitta et al. (10)
JCL307	JCL16 Δ*ldhA* Δ*adhE* Δ*frdBC* Δ*pta* Δ*aceA*	This study
JCL299F	JCL299/pCS138, pEL11, pIM8	Shen et al. (9)
JCL299FT	JCL299/pCS138, pTO1, pIM8	Ohtake et al. (7)
JCL306FT	JCL305/pCS138, pTO1, pIM8	Nitta et al. (10)
JCL307FT	JCL307/pCS138, pTO1, pIM8	This study
Plasmid		
pCS138	$P_L$lacO_1:: *fdh*$_{CB}$ pSC101 *ori* Cm^r	Shen et al. (9)
pEL11	$P_L$lacO_1:: *atoB*$_{EC}$-*adhE2*$_{CA}$-*crt*$_{CA}$-*hbd*$_{CA}$ ColE1 *ori* Amp^r	Shen et al. (9)
pIM8	$P_L$lacO_1:: *ter*$_{TD}$ Cola *ori* Kan^r	Shen et al. (9)
pTO1	$P_L$lacO_1:: *atoB*$_{EC}$-*adhE2*$_{CA}$-*crt*$_{CA}$-*hbd*$_{CA}$ ColE1 *ori* Amp^r (Improved *adhE2*$_{CA}$ RBS strength)	Ohtake et al. (7)
Primer		
RBS lib F	5' – ATGAAAAATTGTGTCATCGTCA GTGC - 3′	Ohtake et al. (7)
RBS lib R	5' – ACGATGACACAATTTTTCATGAT TAACCTCCTCTTTTAT TGSTCTSACCKGGTAAGGTCAGTGCGTC CTGCTG - 3′	Ohtake et al. (7)

CB, *Candida boidinii*; EC, *Escherichia coli*; CA, *Clostridium acetobutylicum*; TD, *Treponema denticola*.

MATERIALS AND METHODS

Reagents Acetic acid, ethanol, $CaCl_2 \cdot 2H_2O$, pyruvic acid, lactate, formic acid, $MgSO_4 \cdot 7H_2O$, kanamycin sulfate, KH_2PO_4, ultrapure-water and chloroform, were purchased from Wako Pure Chemical Industries, Ltd. (Osaka, Japan). 1-Butanol, butanoate, NH_4Cl, Na_2HPO_4, NaCl, D-glucose, IPTG, and thiamine were purchased from Nacalai Tesque (Kyoto, Japan). Yeast extract was purchased from Difco Laboratories (Detroit, MI, USA). Chloramphenicol, ampicillin, tributylamine, phenyl hydrazine hydrochloride, (+)10-camphorsulfonic acid and 1000 × Trace Metal Mix were purchased from Sigma–Aldrich (St. Louis, MO, USA). U–^{13}C labeled dried algal cells were purchased from SI Science (Tokyo, Japan). Methanol was purchased from Kanto Chemical Co., Inc. (Tokyo, Japan).

***E.coli* strains, plasmids and primers** All strains, plasmids and primers used in the study are summarized in Table 1. The metabolic pathway related to the study is shown in Fig. 1.

Medium and cultivation conditions M9 medium (6.8 g Na_2HPO_4, 2 mM $MgSO_4$, 3 g KH_2PO_4, 1 g NH_4Cl, 0.5 g NaCl, 10 mg thiamine, 0.1 mM $CaCl_2$ per liter of water) containing 2 % glucose, 0.5 % yeast extract and 1000 × Trace Metal Mix was used to cultivate *E. coli* strains for metabolome analysis and multivariate analyses using principal component analysis (PCA) and orthogonal projection to latent structures discriminant analysis (OPLS-DA). Pre-cultivation was performed aerobically in M9 + YE medium containing appropriate antibiotics (ampicillin 100 μg/mL, kanamycin 50 μg/mL, chloramphenicol 50 μg/mL) at 37 °C in a rotary shaker (250 rpm) for 17 h. After 17 h of pre-cultivation, an appropriate volume of pre-cultured cells equal to OD_{600} = 0.04 was transferred to a vacutainer tube (10 mL, Becton, Dickinson and Company, Franklin Lakes, NJ, USA) with 4 mL of

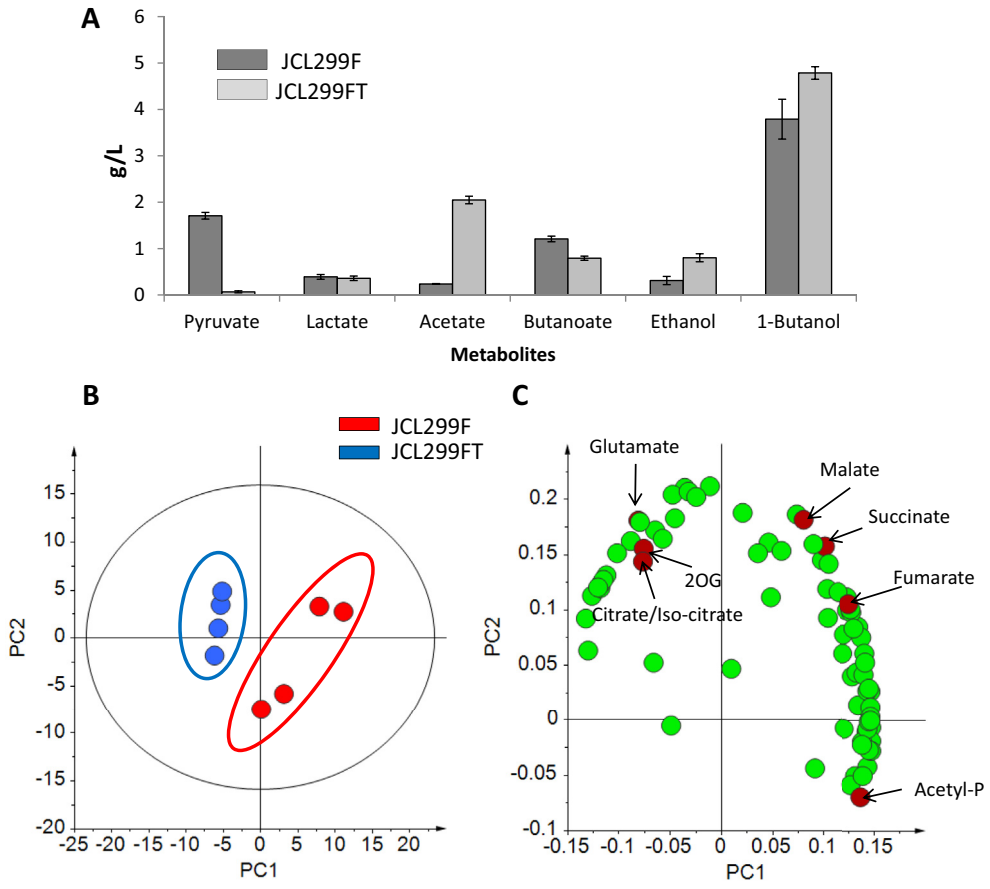

FIG. 2. Metabolome profilie comparison between JCL299F and JCL299FT in M9+YE medium. (A) Fermentation profile of JCL299F and JCL299FT within M9 +YE medium. The cultures were taken after 26 h fermentation. The error bars indicate standard deviations obtained from four replicates. (B) PCA score plot for metabolic profiling of JCL299F and JCL299FT. Auto-scaling was used. PC1 accounts for 58.3% of the total variance and PC2 accounts for 27% of the total variance. The ellipse indicates 95% confidence border based on Hotelling's T^2. (C) Corresponding loading plot which explains the metabolites contribution to separation of two strains. Abbreviations of metabolites are shown in Table S1. All metabolites contribution is shown in Fig. S1.

fresh M9 + YE medium with appropriate antibiotics. Cultures were incubated at 37 °C in a rotary shaker (250 rpm) and induced with 0.1 mM IPTG when the OD_{600} reached 0.4 to 0.6. After the cultures were incubated for 2 h under aerobic condition, cultivation was switched to anaerobic conditions as described previously (10). The cultures were then incubated at 37 °C at 250 rpm for 24 h. Fresh M9 + YE medium containing 1.5% glucose was fed to the culture after 12 h of fermentation inside the anaerobic chamber.

Sampling and extraction for intracellular metabolome analysis Cultured cells were harvested by fast-filtration method as follows: Culture equivalent to 5 OD_{600} units was harvested using a nylon membrane filter (0.45 μm pore size, 47 mm diameter, Millipore, Burlington, MA, USA). A sample was prepared for ion-pair liquid chromatography/tandem mass spectrometry (LC/MS/MS) analysis while another was prepared for aldehydes analysis by LC/MS/MS with derivatization. Samples in 2 mL Eppendorf tubes were submerged in liquid nitrogen for quenching and kept at −80 °C until extraction. Extraction procedure for ion-pair LC/MS/MS was done as previously described (7). The extracted samples were concentrated using a spin dryer (VC−36 S, Taitec, Tokyo, Japan) and freeze dried overnight. The pellet was re-suspended in 100 μL of ultrapure water and centrifuged at 5000 × *g* for 5 min at 4 °C and 40 μL of the sample was transferred to a glass vial for ion-pair LC/MS/MS analysis.

Extracellular metabolites measurement by gas chromatography/flame ionization detector and ultra fast liquid chromatography/photodiode array Culture medium (600 μL) after 24 h cultivation was centrifuged at 16,000 × *g* for 10 min at 4 °C after which the supernatant was collected and filtered using a 0.2 μm pore size PTFE hydrophilic membrane filter (Millipore). Extracellular metabolites measurement was performed using the same protocol as previously reported (7).

Intracellular metabolites analysis by ion-pair LC/MS/MS Ion-pair LC-MS/MS was used to measure intracellular metabolites including central carbon metabolites as previously reported (7). Briefly, Nexera UHPLC coupled with LCMS 8030 Plus (Shimadzu, Kyoto, Japan) was used with an L-column 2ODS (15 cm × 2.1 mm, particle size 3 μm, Chemicals Evaluation and Research Institute, Tokyo, Japan). 10 mM tributylamine with 15 mM acetate in ultra-pure water was used as mobile phase A and methanol was used as mobile phase B. The data file from LC/MS/MS analysis in MRM mode was converted to abf file using Abf file converter (Reifycs Inc., Tokyo, Japan) and all metabolite area values were analyzed by MRMPROBS (12).

Multivariate analysis PCA and OPLS-DA were performed using SIMCA-P+ version 13 (Umetrics, Umea, Sweden). Relative intensities normalized by the area value of (+)-10 camphorsulfonic acid were used as variables.

Glucose consumption measurement The remaining glucose in the culture medium was quantified using the F-kit D-glucose (Roche Diagnostics, Mannheim, Germany) following the manufacturer's instructions.

Preparation of U−^{13}C labeled metabolites U−^{13}C labeled dried algal cells were used to extract U−^{13}C labeled metabolites and 30 mL of mixed-solvent (methanol: ultrapure-water: chloroform; 5:2:2 v/v/v) was added to 150 mg of dried algal cell powder in a 50 mL Falcon tube, vortexed for 30 s and sonicated for 1 min. Three cycles of freezing and thawing were performed (−80 °C until completely frozen and −30 °C until completely thawed). Afterwards, the samples were vortexed for 30 s, sonicated for 1 min and vortexed again for another 30 s. Sample (950 μL) was transferred to 1.5 mL Eppendorf tube and centrifuged at 3500 rpm for 30 min at 4 °C. Ultrapure water (200 μL) was added to the aliquoted solvent, before mixing by vortex for 10 s and centrifugation at 10,000 rpm for 10 min at 4 °C. The polar phase was transferred to a new Eppendorf tube and concentrated using a spin dryer for 2−3 h. The aliquoted solvents were pooled to a new falcon tube and mixed well before transferring 200 μL to a fresh 1.5 mL tube. The samples were freeze-dried overnight and kept at −80 °C freezer until use. Before using the sample as an internal standard, the completeness of ^{13}C-labeling ratio of metabolites was confirmed by the succeeding derivatization and LC/MS/MS analysis procedure.

Extraction and derivatization of glyoxylate The freeze-dried U^{13}C-labeled samples were resuspended in 100 μL of ultrapure water and used as internal

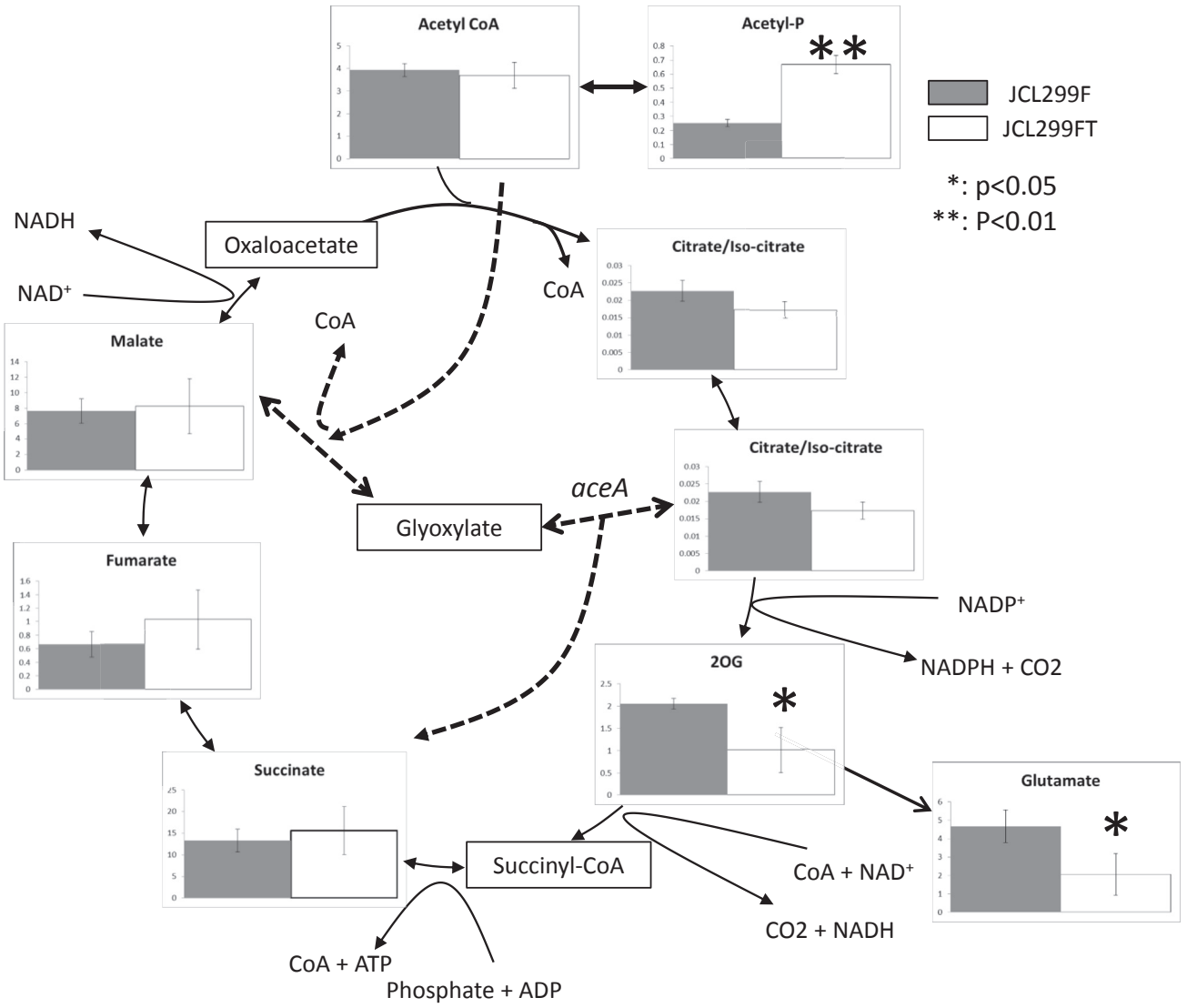

FIG. 3. Metabolite comparison of TCA cycle between JCL299F and JCL299FT. The error bar indicates standard deviations obtained from four replicates. Asterisks indicate significant difference from control strain, JCL299F (*$p < 0.05$, **$p < 0.01$).

standards. The frozen samples were added with 1.8 mL of mixed solvent (methanol:ultrapure-water:chloroform; 5:2:2 v/v/v) with 20 μL of $U^{13}C$-labeled extract and kept at - 30 °C for 1 h. Supernatant (800 μL) was transferred to a new tube and added with 400 μL of ultrapure-water. After centrifugation at 5000 × *g* for 5 min at 4 °C, 400 μL of the upper polar phase was transferred to a new Eppendorf tube and filtrated with a 0.2 μm PTFE hydrophilic membrane filter (Millipore). Afterwards, 0.02 M phenylhydrazine (200 μL) was added to the sample before concentration by spin-drying for 1.5 h. Samples were mixed well with a vortex and 40 μL samples were transferred to LC glass vials.

Glyoxylate analysis by LC/MS/MS Glyoxylate was analyzed by LC/MS/MS in negative ion mode. Nexera UHPLC coupled with LCMS 8050 (Shimadzu) was used with Discovery HS F5-3 column (15 cm × 2.1 mm, particle size 3 μm, Sigma–Aldrich). The mobile phase A was ultra-pure water with 0.1 % (v/v) formate and mobile phase B was acetonitrile. The percentage of mobile phase B was held at 0% for 1 min and raised at the following rates: (i) 80%/min until 40%, (ii) 1.43%/min until 45%, (iii) 55%/min until 100% and held for 2 min, (iv) decreased to 0% in a minute. The flow rate was 3 mL/min, injection volume was 3 μL, probe position was +1.0 mm, temperature of de-solvent line was maintained at 250 °C, temperature of heat block was maintained at 400 °C, temperature of column oven was maintained at 40 °C, nebulizer gas flow rate was 3 L/min and drying gas flow rate was 10 L/min.

The area values of $U-^{12}C$ and $U-^{13}C$ labeled glyoxylate were quantified by Lab Solutions (Shimadzu). To calibrate derivatization efficiency and concentrating efficiency between samples, $U-^{13}C$ labeled metabolite was used as internal standard and relative intensity of glyoxylate were calculated.

RESULTS AND DISCUSSION

Metabolic footprinting of 1-butanol-producing strains cultivated in M9 + YE medium In the previous study, *E. coli* was engineered to produce 1-butanol via the introduction of a modified *Clostridial* CoA-dependent 1-butanol producing pathway. This particular strain, JCL299FT, was able to produce a 1-butanol titer equal to 18.3 g/L in rich (TB) medium by knocking out competing pathways, overexpression of *adhE2 (*encoding for alcohol dehydrogenase) and addition of cysteine to the medium (as precursor of CoA) (Fig. 1) (7–9). However, in terms of cost reduction in the industrial scale, 1-butanol production in lean medium would be preferable. Thus, JCL299FT was cultivated in the lean medium M9 + YE and extracellular metabolites profiling was performed to identify major carbon leaks to pathways that produce by-products. Six extracellular metabolites namely pyruvate, lactate, acetate, butanoate, ethanol and 1-butanol were quantified in JCL299FT grown in M9+YE medium. Since acetate accumulation was observed in the strain grown in M9 + YE (Fig. 2A), decreasing acetate production in the strain is necessary in order to increase 1-butanol production.

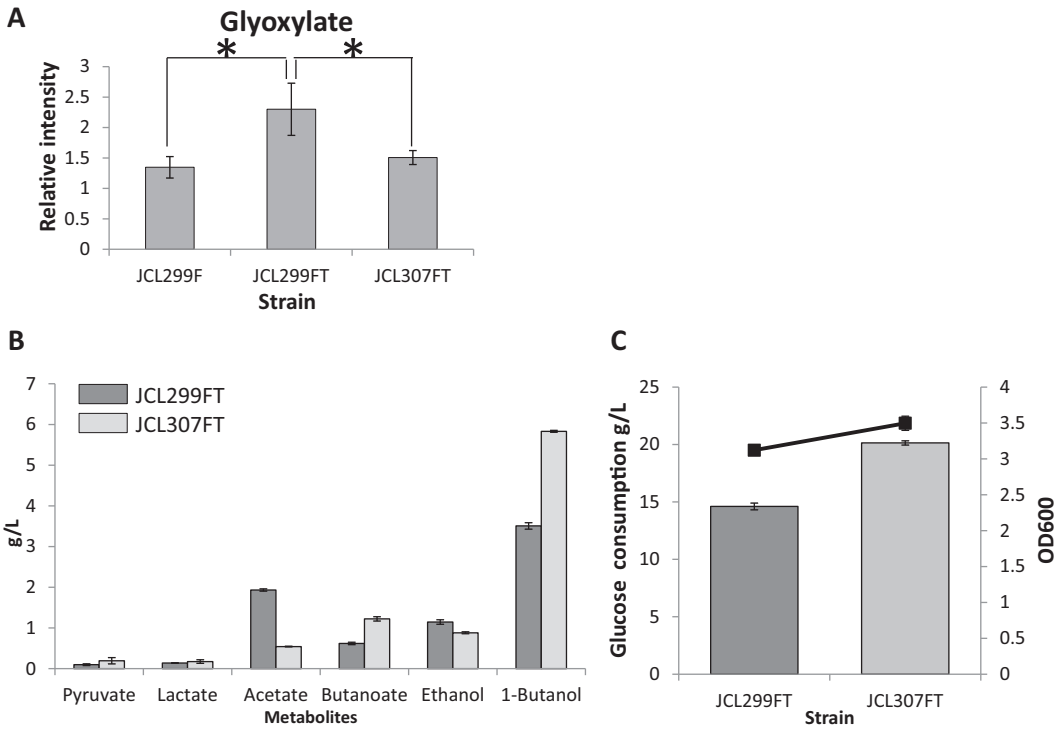

FIG. 4. Comparison of glyoxylate amount, extracellular metabolites, glucose consumption and growth in JCL299FT and JCL307FT. (A) Glyoxylate amount comparison between JCL299F, JCL299FT and JCL307FT. The error bar indicates standard deviations obtained from three replicates. Asterisks indicate significant difference from other strain (*$p < 0.05$). (B) Extracellular metabolites production assay of JCL307FT within M9 + YE medium. The cultures were taken after 24 h fermentation. The error bar indicates standard deviations obtained from three replicates. Each metabolites yields are shown in Fig. S2. (C) Glucose consumption (g/L) and growth (OD_{600}) comparison. Glucose consumption is shown by bar-graph and growth (OD_{600}) is showed by dot chart plot. The cultures were taken after 24 h fermentation. The error bar indicates standard deviations obtained from three replicates.

Acetate accumulation during fermentation has been well studied and several mechanisms for it have been proposed. One mechanism suggests an acetate overflow caused by the imbalance between substrate uptake and anabolic/catabolic reactions of downstream pathways (13) while another mechanism suggests the regeneration of free CoA from acetyl-CoA in order to supply extra ATP in this process. Although we previously decreased acetate production and increased acetyl-CoA (an important precursor of 1-butanol pathway metabolites) by knocking out *eutD*, it caused unexpected pyruvate accumulation and resulted in a decrease in 1-butanol production (10). Thus, effective gene targets other than *eutD* should be identified in order to increase 1-butanol production.

Identification of increased glyoxylate accumulation High-resolution phenotyping by metabolome analysis using ion-pair LC/MS/MS was performed to gain insights into the resulting changes caused by over-expression of *adhE2*. Metabolites including central carbon metabolites, amino acids, nucleosides, nucleotides, nucleobases and cofactors were compared between the non-acetate producing JCL299F and acetate-producing JCL299FT. A total of 74 detected metabolites were subjected to an unsupervised type of multivariate analysis, specifically the principal component analysis (PCA) (Figs. 2B, C, and S1). Result showed that there is separation of the two strains JCL299F and JCL299FT along the right diagonal line between PC1 and PC2.

The metabolites that contributed the most to the separation of the two strains were glutamate and 2OG. Specifically, glutamate and 2OG accumulated in JCL299F while acetyl-phosphate increased in JCL299FT. In JCL299FT, accumulation of acetyl-phosphate, the precursor of acetate, is likely due to the activation of *eutD* (10). When compared to JCL299F, only 2OG and glutamate showed a decrease in JCL299FT while other TCA cycle metabolites did not show any significant changes (Fig. 3). Therefore, we also hypothesized that glyoxylate may have altered concentrations in JCL299FT. To check whether there was a change in the amount of glyoxylate in JCL299FT, the glyoxylate level was analyzed by LC/MS/MS with derivatization. Results showed that a higher amount of glyoxylate was produced in JCL299FT (Fig. 4A). While the glyoxylate shunt is known to be repressed in anaerobic conditions in wildtype strains of *E. coli*, JCL299FT has been extensively engineered to have higher concentrations and flux of acetyl-CoA (10). The resulting perturbations to the TCA cycle may in turn alter this expression, similar to previous works that demonstrate altered glyoxylate shunt expression due to genetic modifications in anaerobic condition (14).

Knocking out *aceA* decreased acetate and increased 1-butanol production in JCL299FT Here we focused on the possible interference of the glyoxylate shunt in further strain modifications because glyoxylate shunt would consume acetyl-CoA that may otherwise be used to increase flux through the 1-butanol pathway. The glyoxylate shunt is a bypass pathway of the TCA cycle and uses iso-citrate lyase and malate synthase encoded by *aceA* and *aceB*, respectively (15), and regulated by a complicated mechanism involving IclR, FadR, IHF, ArcAB and CsrA (16–19). To prevent the possible conversion of acetyl-CoA to glyoxylate shunt, *aceA* was knocked out in JCL299FT (designated as JCL307FT). JCL307FT strain showed a significant decrease in acetate production that led to better growth (higher OD_{600} value), higher glucose consumption and finally, a 39% improvement in 1-butanol production (Fig. 4B). Previous report (11) has shown that acetate accumulation impairs protein biosynthesis and eventually growth. Therefore, decreased accumulation of acetate may be one of the reasons of improved growth of strain JCL307FT. In addition, it is widely known that *E. coli* grows best at pH 7.0 and thus, similar to other *E.coli* BW25113 strain derivatives, the pH of the medium is generally adjusted to 7.0 when

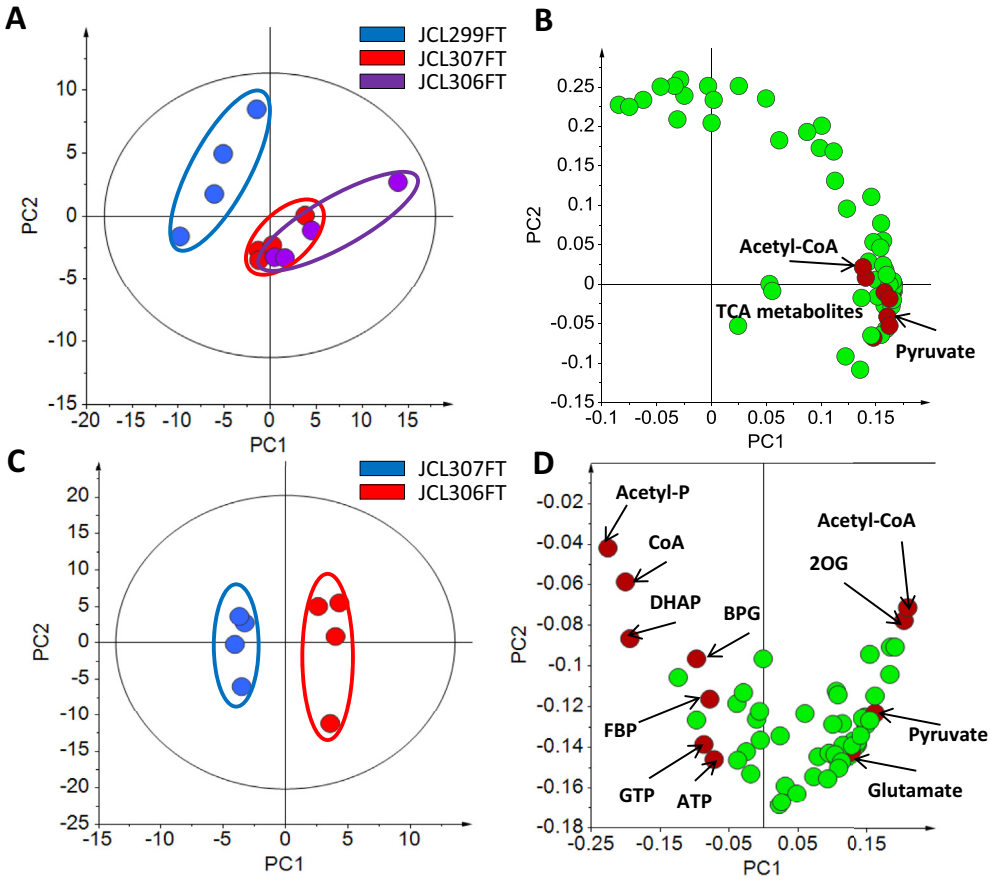

FIG. 5. Metabolome analysis of 3 strains (JCL299FT, JCL306FT and JCL307FT). (A) PCA score plot for metabolic profiling of JCL299FT, JCL306FTFT and JCL307FT. Auto-scaling was used. PC1 accounts for 60.0% of the total variance and PC2 accounts for 24% of the total variance. The ellipse indicates 95% confidence border based on Hotelling's T^2. (B) Corresponding loading plot which explains the metabolites contribution to separation of two strains of panel A. All metabolites contribution is shown in Fig. S6A. (C) OPLS-DA score plot of JCL306FT and JCL307FT. Auto-scaling was used. PC1 accounts for 26.0% of the total variance. The ellipse indicates 95% confidence border based on Hotelling's T^2. (D) Corresponding loading plot which explains the metabolites contribution to separation of two strains of panel C. All metabolites contribution is shown in Fig. S6B.

used for target compound production (8,20–22). We observed that the pH of the culture medium of JCL307FT increased to 6.9 ± 0.1 compared to around 6.0 ± 0.1 in JCL299FT after 24 h of cultivation (Fig. S2). This may also be one plausible reason why strain JCL307FT showed better growth compared to JCL299FT.

By knocking out *aceA*, acetate production decreased by 72% and 1-butanol production improved by 39% (Fig. 4B). Moreover, glucose consumption increased by 27% and growth increased by 10% (Fig. 4C). When 1-butanol production yield was calculated, 12% improvement was observed (Fig. S3). As a further proof to support the results, growth and glucose consumption were compared between the three strains JCL299F, JCL299FT and JCL307FT (Fig. S4). This result showed that the growth and glucose consumption increased with the each successive genetic modification. This also resulted in a stepwise improvement in 1-butanol production as 1-butanol production is coupled to growth (8). In this study, metabolome analysis was performed to check the effect of *aceA* knockout on the metabolome state. Consequently, glyoxylate (Fig. 4A) and acetyl-phosphate, the precursor of acetate, both decreased after knocking out *aceA* (Fig. S5). By removing the glyoxylate shunt, TCA cycle metabolites including 2OG and glutamate increased, which indicates that either carbon siphoning from the TCA cycle decreased or flux to TCA cycle increased (Fig. S5).

Comparative metabolome analysis of *aceA* and *eutD* knockout strains To gain insights on the difference between *aceA* and *eutD* knockout strains, metabolome analysis of the aforementioned strains was conducted (Fig. 5).

Metabolome analysis with PCA showed that the metabolome states of JCL306FT (JCL299FT *ΔeutD*) and JCL307FT (JCL299FT *ΔaceA*) were similar since the two strains overlap in the score plot (Fig. 5A). Specifically, pyruvate and TCA cycle metabolites contributed to the separation of *eutD* knockout and *aceA* knockout strains in PCA loading plot (Figs. 5B and S6A). To find out the difference between the two strains, OPLS-DA model was constructed (Fig. 5C). Consequently acetyl-phosphate, free CoA, ATP, GTP and glycolysis metabolites were plotted on the left side along PC1 while acetyl-CoA, 2OG, pyruvate and glutamate were plotted on the right side along PC1 (Figs. 5D and S6B). Here, the comparison of acetyl-phosphate, free CoA, acetyl-CoA and 2OG amount among the three strains is shown in Fig. 6A while comparison of other metabolites that may be important to the separation between the two strains is shown in Fig. S7. It is worth noting that based on the OPLS-DA, free CoA was found to be significantly different between the *aceA* knockout and *eutD* knockout strains. As can be seen in Fig. 6A, free CoA amount increased significantly in *aceA* knockout while it did not increase in *eutD* knockout strain. In addition, a decrease in acetate production was more pronounced in the *eutD* knockout strain (Fig. S8) and extracellular pyruvate accumulation was observed in only *eutD* knockout strain (Fig. 4B) (10). A summary of the difference between *eutD* knockout strain and *aceA* knockout strain is shown in Table 2. The importance of free CoA availability for 1-butanol production and observation of pyruvate accumulation because of occurrence of free CoA imbalance has been

discussed in previous studies (7,10). The CoA-dependent 1-butanol pathway has been shown to be highly affected by the availability of free CoA. Previously, we demonstrated that increasing the expression of *adhE2* to enhance free CoA recycling was successful in improving titers in JCL299FT (7). In addition, another previous study identified free CoA limitation in JCL299FT strain and cysteine supplementation and over-expression of *atoB*, which encodes acetyl-CoA acetyltransferase to increase free CoA availability succeeded in increasing free CoA amount and improving 1-butanol production (10). Taken together, for unknown reasons the *aceA* knockout was able to increase free CoA amount and bypass acetate overflow while the *eutD* knockout was able to completely eliminate the acetate producing pathway and caused free CoA imbalance, resulting in extracellular pyruvate accumulation. For free CoA generation in *aceA* knockout strain, many reactions should be contributing to increasing free CoA availability, specifically free CoA release via reaction from butyryl-CoA to butanoate, which leads to extracellular butanoate secretion and releases a molecule of free CoA. However, in addition to above specified reactions, other reactions might be contributing to new free CoA balancing in *aceA* knockout strain, which led to improved 1-butanol production.

TABLE 2. Metabolites amount change trend in *eutD* knockout strain and *aceA* knockout strain compared to control strain JCL299FT.

	Metabolite	JCL306FT (Δ*eutD*)	JCL307FT (Δ*aceA*)
Extracellular	Pyruvate	Increased [a]	No significant change [b]
	Acetate	Decreased[c]	Decreased[b]
	1-Butanol	Decreased [a]	Increased[b]
Intracellular	Free CoA	No significant change[d]	Increased[d]

[a] Based on Nitta et al. (10).
[b] See Fig. 4B.
[c] See Fig. S8.
[d] See Fig. 6A.

Nonetheless, many elements of the central carbon metabolism are affected due to the deletion of the glyoxylate shunt besides free CoA availability, including the availability of C4 and C5 compounds, anaplerotic pathways, the TCA cycle, and all metabolites derived from TCA cycle intermediates. Therefore, while free CoA availability may present one reason for the altered phenotype, there are likely other contributing factors.

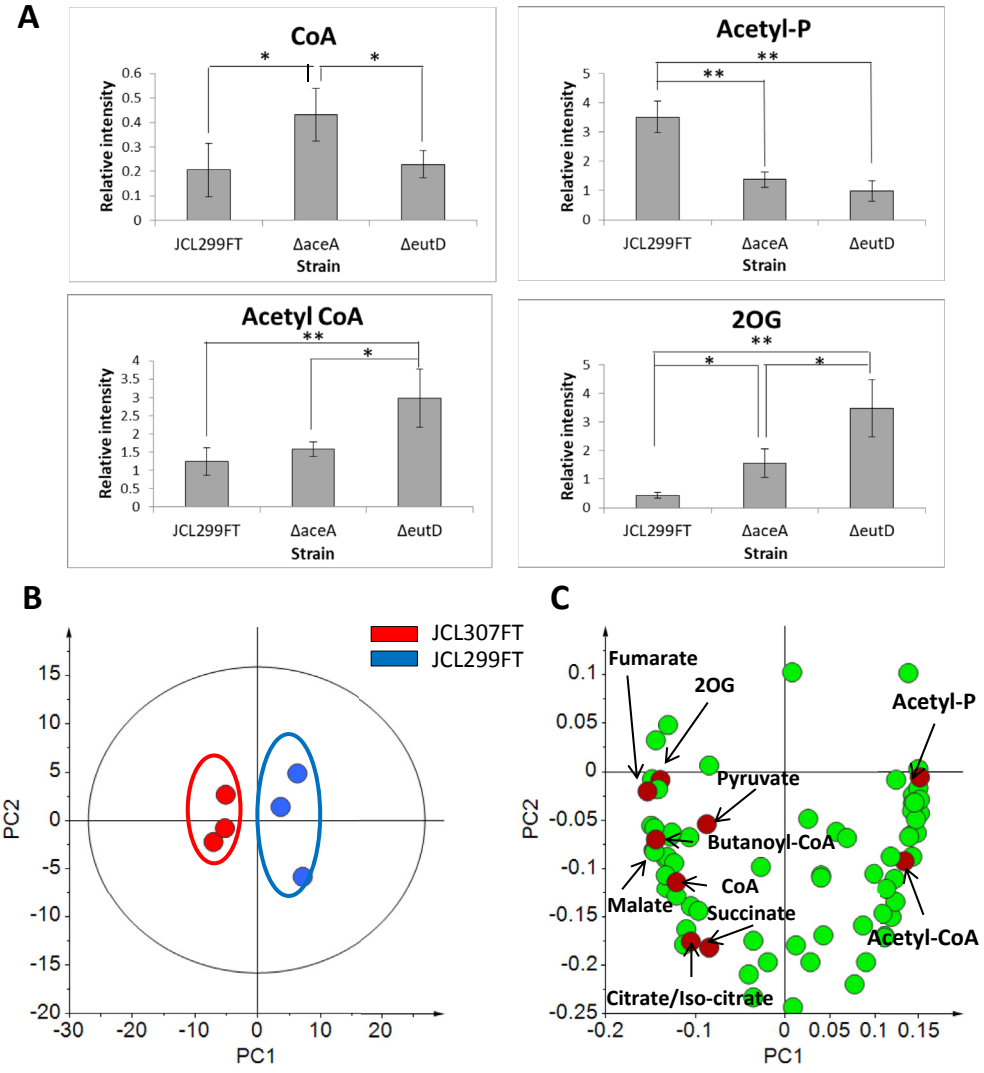

FIG. 6. Glyoxylate amount comparison and PCA plot of JCL299FT and JCL307FT. (A) Amount comparison of four metabolites, which showed the most significant difference between JCL306FT and JCL307FT in OPLS-DA. Here acetyl-phosphate and free CoA is unique in JCL307FT while acetyl-CoA and 2OG is unique in JCL306FT. Error bar means standard deviation from four replicates. Asterisks indicate significant difference from other strain and medium ($^*p < 0.05$, $^{**}p < 0.01$). (B) PCA score plot for metabolic profiling of JCL299FT and JCL307FT. Auto-scaling was used. PC1 accounts for 56.0% of the total variance and PC2 accounts for 20% of the total variance. The ellipse indicates 95% confidence border based on Hotelling's T^2. (C) Corresponding loading plot which explains the metabolites contribution to separation of two strains. All metabolites contribution is shown in Fig. S9.

In addition, to determine why acetate production decreased by knocking out *aceA*, metabolome analysis was performed. PCA analysis of JCL299FT and JCL307FT was conducted to check the major metabolome changes (Fig. 6B, C).

The PCA plot showed that TCA cycle metabolites accumulated in JCL307FT (Figs. 6C and S5). This suggests that the flux to TCA cycle might have increased as indicated in the previous section. It is probable that knocking out the glyoxylate shunt resolved the imbalance between substrate uptake and metabolic activities of downstream pathways, consequently avoiding acetate overflow. This is quite reasonable since flux limitation to TCA cycle is one of the major causes of acetate overflow (23,24).

Cultivation of JCL307FT in rich medium: TB medium In order to evaluate the production ability of JCL307FT in rich medium, production test was done in TB medium. When 1-butanol production yield was calculated as g/g, an increase was observed and JCL307FT showed a yield of 0.37 g/g on average, which is almost the maximum theoretical 1-butanol production yield (0.41 g/g) of this strain (Fig. S10). Interestingly, *aceA* knockout had a greater effect in minimal medium (M9) +YE than in TB medium as indicated by the increased titers. This big improvement in 1-butanol using minimal medium (M9) + YE can be useful for industrial applications as cost reduction can be achieved by using a lean medium. Through this study, the usefulness of metabolome analysis for identification of gene targets for strain improvement in metabolic engineering study was shown.

Supplementary data related to this article can be found at https://doi.org/10.1016/j.jbiosc.2018.08.013.

ACKNOWLEDGMENTS

This research was fully supported by Japan Science and Technology (JST), Strategic International Collaborative Research Program, SICORP for JP-US Metabolomics and National Science Foundation (NSF) MCB-1139318. This study will be included in a dissertation submitted by Katsuaki Nitta to Osaka University in partial fulfillment of the requirement for his doctor degree.

References

1. **Fiehn, O.:** Metabolomics - the link between genotypes and phenotypes, Plant Mol. Biol., **48**, 155–171 (2002).
2. **Gold, N. D., Gowen, C. M., Lussier, F. X., Cautha, S. C., Mahadevan, R., and Martin, V. J. J.:** Metabolic engineering of a tyrosine-overproducing yeast platform using targeted metabolomics, Microb. Cell Fact., **14**, 73 (2015).
3. **Hasunuma, T., Sanda, T., Yamada, R., Yoshimura, K., Ishii, J., Kondo, A., Hahn, H. B., Galbe, M., Gorwa, G. M., and Lidén, G.:** Metabolic pathway engineering based on metabolomics confers acetic and formic acid tolerance to a recombinant xylose-fermenting strain of *Saccharomyces cerevisiae*, Microb. Cell Fact., **10**, 2 (2011).
4. **Korneli, C., Bolten, C. J., Godard, T., Franco, L. E., and Wittmann, C.:** Debottlenecking recombinant protein production in *Bacillus megaterium* under large-scale conditions-targeted precursor feeding designed from metabolomics, Biotechnol. Bioeng., **109**, 1538–1550 (2012).
5. **Teoh, S. T., Putri, S., Mukai, Y., Bamba, T., and Fukusaki, E.:** A metabolomics-based strategy for identification of gene targets for phenotype improvement and its application to 1-butanol tolerance in *Saccharomyces cerevisiae*, Biotechnol. Biofuels, **8**, 144 (2015).
6. **Noguchi, S., Putri, S. P., Lan, E. I., Laviña, W. A., Dempo, Y., Bamba, T., Liao, J. C., and Fukusaki, E.:** Quantitative target analysis and kinetic profiling of acyl-CoAs reveal the rate-limiting step in cyanobacterial 1-butanol production, Metabolomics, **12**, 26 (2016).
7. **Ohtake, T., Pontrelli, S., Laviña, W. A., Liao, J. C., Putri, S. P., and Fukusaki, E.:** Metabolomics-driven approach to solving a CoA imbalance for improved 1-butanol production in *Escherichia coli*, Metab. Eng., **41**, 135–143 (2017).
8. **Atsumi, S., Cann, A. F., Connor, M. R., Shen, C. R., Smith, K. M., Brynildsen, M. P., Chou, K. J. Y., Hanai, T., and Liao, J. C.:** Metabolic engineering of *Escherichia coli* for 1-butanol production, Metab. Eng., **10**, 305–311 (2008).
9. **Shen, C. R., Lan, E. I., Dekishima, Y., Baez, A., Cho, K. M., and Liao, J. C.:** Driving forces enable high-titer anaerobic 1-butanol synthesis in *Escherichia coli*, Appl. Environ. Microbiol., **77**, 2905–2915 (2011).
10. **Nitta, K., Laviña, W. A., Pontrelli, S., Liao, J. C., Putri, S. P., and Fukusaki, E.:** Orthogonal partial least squares/projections to latent structures regression-based metabolomics approach for identification of gene targets for improvement of 1-butanol production in *Escherichia coli*, J. Biosci. Bioeng., **124**, 498–505 (2017).
11. **De, M. M., De, M. S., Soetaert, W., and Vandamme, E.:** Minimizing acetate formation in *E. coli* fermentations, J. Ind. Microbiol. Biotechnol., **34**, 689–700 (2007).
12. **Tsugawa, H., Arita, M., Kanazawa, M., Ogiwara, A., Bamba, T., and Fukusaki, E.:** MRMPROBS: a data assessment and metabolite identification tool for large-scale multiple reaction monitoring based widely targeted metabolomics, Anal. Chem., **85**, 5191–5199 (2013).
13. **Castaño, C. S., Pastor, J. M., Renilla, S., Bernal, V., Iborra, J. L., and Cánovas, M.:** An insight into the role of phosphotransacetylase (*pta*) and the acetate/acetyl-CoA node in *Escherichia coli*, Microb. Cell Fact., **8**, 54 (2009).
14. **Sanchez, A. M., Bannett, G. N., and San, K. Y.:** Novel pathway engineering design of the anaerobic central metabolic pathway in *Escherichia coli* to increase succinate yield and productivity, Metab. Eng., **7**, 229–329 (2005).
15. **Maharjan, R. P., Yu, P. L., Seeto, S. A., and Ferenci, T.:** The role of isocitrate lyase and the glyoxylate cycle in *Escherichia coli* growing under glucose limitation, Res. Microbiol., **156**, 178–183 (2005).
16. **Cronan, J. E., Jr. and Laporte, D.:** Tricarboxylic acid cycle and glyoxylate bypass, EcoSal Plus, **1**, https://doi.org/10.1128/ecosalplus.3.5.2 (2005).
17. **Cozzone, A. J.:** Regulation of acetate metabolism by protein phosphorylation in enteric bacteria, Annu. Rev. Microbiol., **52**, 127–164 (1998).
18. **Romeo, T.:** Global regulation by the small RNA-binding protein CsrA and the non-coding RNA molecule CsrB, Mol. Microbiol., **29**, 1321–1330 (1998).
19. **Wei, B., Shin, S., Laporte, D., Wolfe, A. J., and Romeo, T.:** Global regulatory mutations in *csrA* and *rpoS* cause severe central carbon stress in *Escherichia coli* in the presence of acetate, J. Bacteriol., **182**, 1632–1640 (2000).
20. **Chen, G. S., Siao, S. W., and Shen, C. R.:** Saturated mutagenesis of ketoisovalerate decarboxylase V461 enabled specific synthesis of 1-pentanol via the ketoacid elongation cycle, Sci. Rep., **7**, 11284 (2017).
21. **Yim, H., Haselbeck, R., Niu, W., Pujol-Baxley, C., Burgard, A., Boldt, J., Khandurina, J., Trawick, J. D., Osterhout, R. E., Stephen, R., and other 8 authors:** Metabolic engineering of *Escherichia coli* for direct production of 1,4-butanediol, Nat. Chem. Biol., **7**, 445–452 (2011).
22. **Liang, K. and Shen, C. R.:** Engineering cofactor flexibility enhanced 2,3-butanediol production in *Escherichia coli*, J. Ind. Microbiol. Biotechnol., **44**, 1605–1612 (2017).
23. **Peebo, K., Valgepea, K., Nahku, R., Riis, G., Õun, M., Adamberg, K., and Vilu, R.:** Coordinated activation of PTA-ACS and TCA cycles strongly reduces overflow metabolism of acetate in *Escherichia coli*, Appl. Microbiol. Biotechnol., **98**, 5131–5143 (2014).
24. **Veit, A., Polen, T., and Wendisch, V. F.:** Global gene expression analysis of glucose overflow metabolism in *Escherichia coli* and reduction of aerobic acetate formation, Appl. Microbiol. Biotechnol., **74**, 406–421 (2007).